AIP | The Journal of Chemical Physics

Full-dimensional quantum calculations of the vibrational states of H5+

Hongwei Song, Soo-Ying Lee, Minghui Yang, and Yunpeng Lu

Citation: J. Chem. Phys. **138**, 124309 (2013); doi: 10.1063/1.4797464
View online: http://dx.doi.org/10.1063/1.4797464
View Table of Contents: http://jcp.aip.org/resource/1/JCPSA6/v138/i12
Published by the American Institute of Physics.

Full-dimensional quantum calculations of the vibrational states of H_5^+

Hongwei Song,[1] Soo-Ying Lee,[1] Minghui Yang,[2,a)] and Yunpeng Lu[1,a)]
[1]*Division of Chemistry and Biological Chemistry, School of Physical and Mathematical Sciences, Nanyang Technological University, Singapore 637371, Singapore*
[2]*Key Laboratory of Magnetic Resonance in Biological Systems, State Key Laboratory of Magnetic Resonance and Atomic and Molecular Physics, Wuhan Centre for Magnetic Resonance, Wuhan Institute of Physics and Mathematics, Chinese Academy of Sciences, Wuhan 430071, People's Republic of China*

(Received 27 November 2012; accepted 11 March 2013; published online 28 March 2013)

Full-dimensional quantum calculations of the vibrational states of H_5^+ have been performed on the accurate potential energy surface developed by Xie *et al.* [J. Chem. Phys. **122**, 224307 (2005)]. The zero point energies of H_5^+, H_4D^+, D_4H^+, and D_5^+ and their ground-state geometries are presented and compared with earlier theoretical results. The first 10 low-lying excited states of H_5^+ are assigned to the fundamental, overtone, and combination of the H_2–H_3^+ stretch, the shared proton hopping and the out-of-plane torsion. The ground-state torsional tunneling splitting, the fundamental of the photon hopping mode and the first overtone of the torsion mode are 87.3 cm^{-1}, 354.4 cm^{-1}, and 444.0 cm^{-1}, respectively. All of these values agree well with the diffusion Monte Carlo and multi-configuration time-dependent Hartree results where available. © *2013 American Institute of Physics*. [http://dx.doi.org/10.1063/1.4797464]

I. INTRODUCTION

The ionic hydrogen clusters, H_{2n+1}^+ (with $n > 1$), are of key relevance for modeling planetary atmospheres and interstellar clouds, for understanding the mechanism of ion-solvent interaction, and for applications as a possible medium for energy storage.[1–5] As the first member of this series, H_5^+ has attracted considerable attention both experimentally[6–23] and theoretically,[23–51] mainly due to its unusual fluxionality, which violates the conventional chemical picture of a structure being given by an equilibrium structure.

H_5^+ was first observed by Dawson and Tickner[6] in the negative glow of a hydrogen electric discharge in 1962. Many experimental efforts have been paid to the determination of dissociation enthalpies and entropies for the $H_3^+ + H_2 \rightarrow H_5^+$ clustering reaction,[7–13] vibrational fundamental frequencies,[14,15] and rate coefficients at typical interstellar clouds temperatures.[16–20] Until recently, Cheng *et al.*[22] reported a comparison of theoretical and experimental dissociation infrared (IR) spectra in the 2000–4500 cm^{-1} region in which the central proton hopping was shown to have clear spectroscopic signatures. Shortly afterwards, they extended the spectra for H_5^+ and D_5^+ to the mid- and far-IR region of 300–2200 cm^{-1} using resonance-enhanced multiple-photon dissociation and the FELIX free electron laser.[23] The bands were assigned to combinations of the proton hopping, bending, and torsional vibrations.

Theoretical work on H_5^+ started with the investigations on its equilibrium structures, which is remarkably challenging due to the extremely flat and anharmonic features of the potential energy surface (PES) and the significant quantum effects of light nuclei.[35] Numerous *ab initio* calculations have been carried out to determine the saddle points and equilibrium structures,[24–27,29,30,32,35,36,41,42] dissociation energies,[31,52] and low-lying bound and quasi-bound vibrational energies.[28,37–39,45] In addition, several studies of the $H_3^+ + H_2$ reaction and its isotopic analogs have been reported.[34,47–50] These pioneering works showed that there exist 10 stationary points on the PES of H_5^+ and the global minimum refers to an isosceles H_3^+ bound to an H_2 within a C_{2v} arrangement. The next three low-lying stationary points correspond to transition states for the proton hopping (D_{2d} and D_{2h} for the non-planar and planar configurations) and the out-of-plane torsion (C_{2v}). The benchmark CC-R12 calculations showed that the three stationary points are all lying within an energy range of 182.2 cm^{-1} above the global minimum.[30] The other six stationary points have relatively high energies, ranging from 1526.8 cm^{-1} to 2873.2 cm^{-1} by the coupled-cluster method with single and double and perturbative triple excitations (CCSD(T)) with respect to the global minimum.[36] Thus, H_5^+ is expected to be delocalized and the quantum effect should be included when one deals with such a floppy cation.

The construction of PESs of pentatomic and larger polyatomic systems is undoubtedly a complicated and demanding theoretical task. Accurate PESs can be obtained either by fitting the parameters of analytical functions to available high resolution spectroscopic data, or by performing state-of-art *ab initio* calculations for numerous configurations. Based on the diatoms-in-molecules method, Prosmiti *et al.*[32] reported the first global PES of H_5^+ using limited *ab initio* energies and thus it is not very accurate. Moyano and Collins[34] constructed a PES with an average deviation of 175 cm^{-1} on a sparse set of data points using MP2 perturbation theory by a modified Shepard interpolation. Recently, Xie *et al.*[36] built a more accurate PES with an average deviation of 58 cm^{-1}, which was fitted to roughly 100 000

a)Electronic addresses: yangmh@wipm.ac.cn and yplu@ntu.edu.sg

different geometries using the CCSD(T) method and an aug-cc-pVTZ basis set. This PES has full permutational symmetry with respect to interchange of H atoms. Aguado *et al.*[40] developed a triatoms-in-molecules approach and constructed a new PES, which allows a very accurate description of the asymptotic region. In addition, a density functional theory-based PES has also been reported by Barragán *et al.*[52] using B3(H) functional. This surface has very good global behavior, however, it is limited to "on the fly" dynamical calculations.

A number of theoretical works have been presented for the bound states and/or spectroscopies for H_5^+. Acioli *et al.*[39] performed diffusion Monte Carlo (DMC) calculations, with and without importance sampling, predicting a D_{2d} geometry for the zero-point averaged structure of H_5^+ with one H atom "in the middle" between two H_2 diatoms. Furthermore, Tudela *et al.*[41] carried out path integral Monte Carlo (PIMC) "on the fly" calculations and found that the vibrational ground state of H_5^+ is a mixture of its four low-lying structures, and not only of the D_{2d} one. Valdés *et al.*[45] carried out a full-dimensional (FD) quantum dynamics study of the H_5^+ cluster using the multi-configuration time-dependent Hartree (MCTDH) method. The potential operator is constructed as an *n*-mode representation based on a 5-mode combination scheme. They reported FD quantum dynamics results on the first 20 vibrational energies and states of H_5^+ and the properties of these states were analyzed. Later, the same group[46] revisited the vibrational dynamics of H_5^+ and extended their studies to its isotopologues employing the same method but using a different mode combination scheme (4-mode combination scheme). In the MCTDH approach, the PES represented in the *n*-mode representation can accurately describe the configurations in the neighborhood of the chosen reference geometry. However, for the highly anharmonic and fluxional H_5^+ cation, it may doubt that the *n*-mode representation can give a complete description of the features of the bound states. Also, Aguado *et al.*[51] calculated the IR predissociation spectra of H_5^+ using reduced two-dimensional (2D) and three-dimensional (3D) simulations and found that the main peaks in the 3D case are in agreement with the peaks in the experimental spectrum. Very recently, Lin and McCoy[53] performed DMC calculations of H_5^+ and D_5^+ and provided alternative assignments of the infrared multiphoton dissociation spectra.[23] Progressions of transitions in the shared-proton hopping mode with up to nine quanta of excitation were assigned in their results.

In this work, we performed FD quantum calculations of the vibrational levels of H_5^+ and the zero point energies of its isotopologues. The PES of Xie *et al.*[36] was employed for comparison reasons as most of the earlier studies have employed this PES. The calculated results were compared with earlier theoretical work. Since the treatment of the vibrations of H_5^+ does not include any dynamical approximation, the converged FD eigenstates are numerically exact. So our work complement to the previous calculations on the same system. This work is organized as following: In Sec. II, the theoretical methodology employed in our study is outlined; Sec. III presents results and discussions, and a summary is given in Sec. IV.

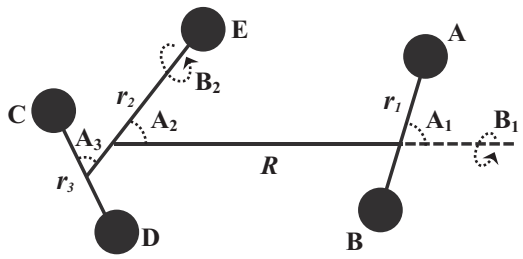

FIG. 1. The Jacobi coordinates for AB-ECD system. R is the distance from the center-of-mass of AB to the center-of-mass of ECD, r_1 is the bond distance of AB, r_2 is the distance between E and the center-of-mass of CD, r_3 is the bond distance of CD, A_1 is the bending angle between R and r_1, A_2 is the bending angle between R and r_2, A_3 is the bending angle between r_2 and r_3, B_1 is the torsion angle around R and B_2 is the torsion angle around r_2.

II. THEORY

The FD Hamiltonian in the body-fixed Jacobi coordinates shown in Fig. 1 for a given total angular momentum J can be written as[54]

$$\hat{H} = \hat{H}_0(R) + \hat{H}_1(r_1) + \hat{H}_2(r_2) + \hat{H}_3(r_3) + \frac{(\hat{J} - \hat{j}_{123})^2}{2\mu R^2} + \frac{\hat{j}_1^2}{2\mu_1 r_1^2} + \frac{\hat{l}_2^2}{2\mu_2 r_2^2} + \frac{\hat{j}_3^2}{2\mu_3 r_3^2} + \hat{V}(R, r_1, r_2, r_3, A_1, A_2, A_3, B_1, B_2), \quad (1)$$

where μ is the reduced mass of AB + ECD, $\hat{J}$ is the total angular momentum operator, $\hat{j}_1$ and $\hat{j}_3$ are the rotational angular momentum operators of AB and CD, and $\hat{l}_2$ is the orbital angular momentum operator of atom E with respect to CD. A_1, A_2, A_3 are the Jacobi angles formed by R and r_1, R and r_2, r_2 and r_3. B_1 is the torsional angle between the plane (R, r_1) and (R, r_2). B_2 is the torsional angle between the plane (R, r_2) and (r_2, r_3). The zeroes of the two dihedral angles B_1 and B_2 are defined as to form a coplanar configuration. $\hat{H}_0(R)$, $\hat{H}_1(r_1)$, $\hat{H}_2(r_2)$, and $H_3(r_3)$ are one-dimensional (1D) reference Hamiltonians. The corresponding eigenstates are denoted as $\phi_{v_0}(R)$, $\phi_{v_1}(r_1)$, $\phi_{v_2}(r_2)$, and $\phi_{v_3}(r_3)$, and

$$\hat{H}_i\phi_{v_i} = [\hat{K}_i + \hat{V}_i]\phi_{v_i} = \epsilon_{v_i}\phi_{v_i} \quad (i = 0 - 3), \quad (2)$$

where $\hat{V}_0(R)$, $\hat{V}_1(r_1)$, $\hat{V}_2(r_2)$, and $\hat{V}_3(r_3)$ are the 1D reference potentials.

The wave function of the system is expanded in terms of the body-fixed (BF) rovibrational eigenfunctions as

$$\psi(\mathbf{R}, \mathbf{r}_1, \mathbf{r}_2, \mathbf{r}_3) = \sum_{v,j,K} F_{vjK}^{JM\epsilon}\phi_{v_0}(R)\phi_{v_1}(r_1)\phi_{v_2}(r_2)\phi_{v_3} \times (r_3)Y_{jK}^{JM\epsilon}(\hat{R}, \hat{r}_1, \hat{r}_2, \hat{r}_3), \quad (3)$$

where v denotes (v_0,v_1,v_2,v_3), j denotes (j_1,l_2,j_3,j_{23},j_{123}). And the potential optimized discrete variable representation (PODVR) technique were employed for the three radial degree-of-freedom in the evaluation of potential energy matrix.[55]

TABLE I. Numerical parameters used in the full-dimensional quantum bound state calculations of H_5^+ and its isotopic variants. The range of B_1 can be reduced from $[0, 2\pi]$ to $[0, \pi]$ according to the space inversion symmetry of the whole system. (Atomic units are used unless stated otherwise.)

Basis/grid	Grid range	Number of basis/grid		Type of basis/ Gauss quadrature
		H_5^+	H_4D^+, D_4H^+, D_5^+	
R	[2.0, 7.0]	12	10	PODVR
r_1	[0.5, 3.0]	3	3	PODVR
r_2	[0.5, 4.5]	18	16	PODVR
r_3	[0.5, 3.0]	5	5	PODVR
j_1/A_1	$[0, \pi/2]$	12/7	16/9	Legendre
j_{23}/A_2	$[0, \pi]$	16/17	20/21	Lobatto
j_3/A_3	$[0, \pi]$	12/13	16/17	Legendre
l_2/B_1	$[0, \pi]$	20/13	24/17	Chebyshev
j_{123}/B_2	$[0, 2\pi]$	24/25	28/33	Chebyshev

The $Y_{jK}^{JM\epsilon}$ in Eq. (3) is the coupled BF total angular momentum eigenfunctions[56] which can be written as

$$Y_{jK}^{JM\epsilon} = (1+\delta_{K0})^{-1/2}\sqrt{\frac{2J+1}{8\pi}}\left[D_{K,M}^{J*}Y_{j_1 j_{23} l_2 j_3}^{j_{123}K} + \epsilon(-1)^{j_1+l_2+j_3+j_{123}+J} D_{-K,M}^{J*}Y_{j_1 j_{23} l_2 j_3}^{j_{123}-K}\right], \quad (4)$$

where $D_{K,M}^J$ is the Wigner rotation matrix, K is the projection of total angular momentum on the body-fixed axis, and $Y_{j_1 j_{23} l_2 j_3}^{j_{123}K}$ is the angular momentum eigenfunction of $\hat{j}_{123}$ defined as

$$Y_{j_1 j_{23} l_2 j_3}^{j_{123}K} = \sum_{\omega} \langle j_1 \omega j_{23} K - \omega | j_{123} K \rangle \, y_{j_1\omega}(\mathbf{r_1}) Y_{j_{23}K-\omega}(\hat{r}_2, \hat{r}_3) \quad (5)$$

and

$$Y_{j_{23}K-\omega}(\hat{r}_2, \hat{r}_3) = \sum_m D_{K-\omega m}^{j_{23}}(\hat{r}_2)\sqrt{\frac{2l_2+1}{2j_{23}+1}} \times \langle j_3 m l_2 0 | j_{23} m \rangle \, y_{j_3 m}(\hat{r}_3), \quad (6)$$

where $y_{j_3 m}$ are spherical harmonics. Note the restriction that $\epsilon(-1)^{j_1+l_2+j_3+j_{123}+J}=1$ for $K=0$ in Eq. (4).

The PARPACK software package[57] has been utilized to calculate the bound states with our own subroutine to perform matrix vector multiplication. It is well known that the kinetic energy matrix (except for the centrifugal potential) is diagonal in the finite basis representation (FBR) and the potential matrix is diagonal in the discrete variable representation (DVR). In order to ensure an efficient matrix vector multiplication, the full-dimensional Hamiltonian is discretized in terms of a PODVR for the four radial coordinates and coupled spherical harmonics for the angular coordinates. In practical calculations, the action of the full-dimensional Hamiltonian on the wave function is divided into three steps: (1) the trial wave function is multiplied by the kinetic energy operator matrix; (2) the trial wave function is transformed to DVR and multiplied by the potential energy surface matrix, and the result is then transformed back to FBR; (3) the results from steps (1) and (2) are summed. These three steps are repeated until the final result is converged. We have also taken advantage of the parity of system and the exchange symmetry of the two atoms of H_2 moiety in H_5^+ whenever possible. The vibrational energy states can be grouped into four symmetry blocks which correspond to four different combinations of the parity and the exchange symmetry.

III. RESULTS

A. Numerical parameters and convergence

The proton scrambling will take place with relatively high energy (the barrier height is ca. 1550 cm^{-1}), in which the central proton changes from H_E to H_C or H_D (see Fig. 1) and vice versa. Due to the huge demand on computation, the current work can only study the energy spectrum up to 774.3 cm^{-1}, which is below the proton scrambling excitation mode. Table I shows the basis/grid number for each of the nine coordinates in our calculations. PODVR basis was used for the four radial coordinates R, r_1, r_2, and r_3. For the angular coordinates A_1 and A_3, Gauss-Legendre quadrature was employed. For the coordinate A_2, to deal with the significant distribution of wave function at $A_2 = 0$, Gauss-Lobatto quadrature[58] was employed because the Gauss-Lobatto integration points include the end points of the integration interval. Gauss-Chebyshev quadrature was employed for the coordinates B_1 and B_2. The range of B_1 can be reduced from $[0, 2\pi]$ to $[0, \pi]$ due to the space inversion symmetry of the whole system. After considering the parity and the exchange symmetry of the hydrogen atoms in the H_2 moiety, the size of the angular basis functions is 77 776 and the number of the grid points for integration of the angular coordinates is 502 775, resulting in a total of 2.5×10^8 basis functions and 1.6×10^9 grid points. The potential cut-off technique was employed to save the computing cost in this work. The cut-off energy was taken to be 25 000 cm^{-1} in the calculations with the points above it being replaced by the cut-off energy. This technique helps to decrease the number of the effective potential energy points from 1.7×10^9 to 8.2×10^8. All the calculations were performed on a distributed-memory cluster with 80 cores (Intel(R) Xeon(R) CPU E5540 @ 2.53GHz). The memory cost is 120 GB for the bound state calculations of H_5^+ and 280 GB for the zero point energy (ZPE) calculation of each of its isotopic variants H_4D^+, D_4H^+, and D_5^+. 8418 matrix-vector products are required to converge the results of H_5^+, and it takes about 28 h for the computation. For

TABLE II. Convergence of the vibrational energies (in cm^{-1}) of H_5^+ with respect to basis/grid number. The angular basis number are first tested in a five-dimensional (5D) model, in which all the radial coordinates are fixed at the global minimum of the PES. Then, the radial basis number are tested in the full-dimensional (FD) model.

5D			
Angular basis no. (j_1,j_{23},j_3,l_2,j_{123})	$n'=0$	$n'=4$	$n'=9$
(10,12,10,22,22)	2433.16	3699.11	4310.68
(10,14,10,24,24)	2432.84	3697.83	4305.19
(12,16,12,28,28)	2432.83	3695.46	4304.17
(20,24,20,44,44)	2432.82	3695.37	4304.12
(12,16,12,20,24)[a]	2432.83	3695.46	4304.17
FD			
Radial basis no. (R,r_1,r_2,r_3)	$n=0$ (ZPE)	$n=5$	$n=8$
(8,3,6,3)	7222.21	7668.57	8056.68
(10,6,8,6)	7220.29	7667.62	7951.40
(10,3,10,5)	7214.92	7661.74	7876.83
(12,3,10,5)	7215.08	7661.90	7872.62
(12,3,14,5)	7214.72	7661.52	7863.07
(12,3,18,5)[a]	7214.63	7661.43	7857.26
(12,3,22,5)	7214.61	7661.40	7854.42
(12,5,18,5)	7214.70	7661.56	7856.90

[a]The results are calculated with these parameters.

the cation D_5^+, 4317 matrix-vector products are required with a computation time of 52 h approximately.

Numerous tests in the vibrational energy calculations of H_5^+ and D_5^+ are shown in Tables II and III, respectively. To settle the converged parameters for the angular basis in calculation for H_5^+, we first carried out a set of testing calculations within a five-dimensional (5D) model, in which the four radial coordinates were fixed at their values in the global minimum (the C_{2v} structure) in the PES. It can be seen from Table II that we achieved a good convergence of less than 0.1 cm^{-1} for the 5D calculations. Then, we employed the angular basis number obtained in the 5D model to perform FD calculations to test the radial basis number and the result are reported in the same table. The vibrational energies for $n=0$ and $n=5$ converge to less than 0.2 cm^{-1} and the vibrational energy for $n=8$ converges to less than 3.0 cm^{-1}. For the D_5^+ cation shown in Table III, it can be found the ZPE converges to less than 1.0 cm^{-1}. Overall, the results presented here are well converged with respect to these parameters.

TABLE III. Convergence of the ZPE values (in cm^{-1}) of D_5^+ with respect to basis/grid number.

FD	
Basis no. (R,r_1,r_2,r_3,j_1,j_{23},j_3,l_2,j_{123})	$n=0$ (ZPE)
(12,3,18,5,12,16,12,20,24)	5155.82
(12,3,18,5,14,18,14,22,26)	5153.10
(12,3,18,5,16,20,16,24,28)	5152.31
(14,3,20,5,12,16,12,20,24)	5155.86
(10,3,16,5,14,18,14,22,26)	5153.07
(10,3,16,5,16,20,16,24,28)[a]	5152.28

[a]Parameters used in the full-dimensional calculations.

B. Ground state properties

The calculated ZPEs of H_5^+ and its isotopic variants, together with other theoretical results reported earlier, are presented in Table IV. All of these calculations employed the same PES of Xie *et al.*[36] except the one used by Cheng *et al.*[22] which is a re-fit to the data reported in Ref. 36 with very small differences. For H_5^+, the ZPE was also computed by the DMC,[22,36,39,53] MULTIMODE "reaction path" (MM-RPH)[22,59–61] PIMC,[41] and MCTDH[45,46] methods. As shown in the third column of Table IV, all values are in good agreement with each other except the one calculated by the MM-RPH method, which is about 30 cm^{-1} higher than others. If we consider the DMC value of Xie *et al.*[36] as the accurate value within statistical error, all the other calculated ZPEs except the MM-RPH one are well located in the statistical error range of the DMC energy. For D_5^+, the three different DMC calculations[22,39,53] gave almost the same ZPE within the statistical uncertainties. The MCTDH ZPE in Ref. 46 and our ZPE agree well with these DMC values. However, the MM-RPH ZPE is higher than the others by at least 20 cm^{-1}. The calculations on the other two isotopomers, H_4D^+ and D_4H^+, were based on the symmetric geometries, in which, the deuteron and the proton, respectively, is in between the two diatoms. For H_4D^+, the ZPE of this work is the same as the value from the DMC without important sampling calculations,[39] while both of them are ca. 8 cm^{-1} larger than the value from the DMC with important sampling calculations. The MCTDH ZPE in Ref. 46 slightly smaller than the other ones and is outside of the statistical uncertainties of the DMC energies. For D_4H^+, the ZPES obtained from DMC[39] (with and without important sampling), MCTDH[46] and this work agree with each other very well.

Almost all high-level *ab initio* studies predicted an asymmetric C_{2v} structure as the energetically lowest stationary point. The DMC calculations showed that the zero-point averaged structure of H_5^+ corresponds to a symmetric D_{2d} geometry.[39] But recent PIMC "on the fly" calculations found that its vibrational ground state is not just the D_{2d} but a mixture of the four low-lying structures.[41] In order to clarify it, we present the one-dimensional probability distribution functions (PDFs) calculated from the ground state wave function of H_5^+ along the coordinates R, r_2, and B_1 in Fig. 2. From the top and middle panels of this figure, it can be seen that the PDF spreads in the range of 3.0 to about 4.75 a.u. in R and simultaneously in a very large region of r_2, which indicates that the central proton is hopping with very large amplitude in between the two outer diatoms. On the other hand, the wave function has nearly the same probability density over the whole range of B_1, which reveals that the H_2 subunit rotates almost freely in the ground state. While calculated average bond lengths of the ground state of H_5^+ showed that the average structure has D_{2d} symmetry, the PDFs of the ground state wave function indicates that the ground state is a mixture of low-lying structures.

C. Assignment of vibrational states

The quantum number assignment of excited states of systems with three or more coupled, anharmonic large

TABLE IV. Comparison of zero point energy (ZPE) values of H_5^+ and its isotopic variants with other theoretical results. (The ZPE values are in cm^{-1} and relative to the potential minimum. In H_4D^+ and D_4H^+, the D and H atom, respectively, is in between the two diatoms.)

		H_5^+	D_5^+	H_4D^+	D_4H^+
Xie *et al.*[a]	DMC	7210 ± 11			
Acioli *et al.*[b]	DMC/IS	7208 ± 4	5151 ± 1	6860 ± 1	5533 ± 2
	DMC/NIS	7213 ± 9	5154 ± 7	6868 ± 11	5535 ± 7
Cheng *et al.*[c]	DMC	7210	5152		
	MM-RPH	7244	5174		
Tudela *et al.*[d]	PIMC	7204.9			
Valdés *et al.*[e]	MCTDH	7210.3			
Valdés *et al.*[f]	MCTDH	7202.6	5151.0	6854.1	5535.6
Lin *et al.*[g]	DMC	7205 ± 5	5149 ± 5		
This work	FD	7214.6	5152.3	6868.8	5536.4

[a]Reference 36.
[b]Reference 39. IS: Importance sampling; NIS: No importance sampling.
[c]Reference 22.
[d]Reference 41.
[e]Reference 45.
[f]Reference 46.
[g]Reference 53.

amplitude motion vibrations is nontrivial.[62,63] The high dimensionality and unusual fluxionality of H_5^+ make the assignment of its vibrational states a challenging task. Due to the existence of low-frequency modes and the strong anharmonic effect, it is difficult to unambiguously label all the calculated eigenstates. For the low-lying states, the coupling between different modes is relatively weak and so the assignments are reliable. Thus, we succeeded in assigning the first 10 excited states of H_5^+, as shown in Table V, by inspecting numerous cuts through the wave function for each state. The assignments are given in terms of three quantum numbers (n_{str}, n_{hop}, n_{tor}), which denote the H_2–H_3^+ stretch, the shared-proton hopping, and the out-of-plane torsion, respectively. This is based on the fact that the other modes have not been excited for those states as they span only a relatively low energy region from 0 to 774.3 cm^{-1} (with respect to the ZPE of H_5^+). The assignment here follows the work of Valdés *et al.* in which the parity has also been included.[45]

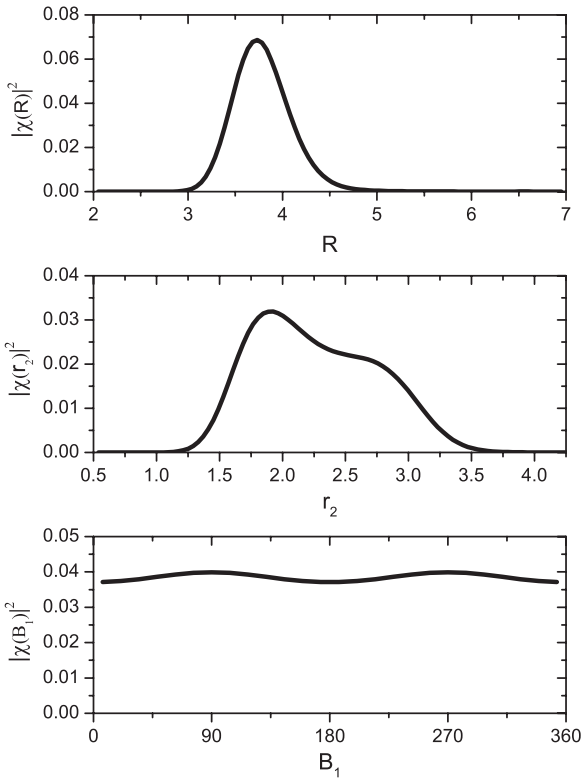

FIG. 2. One-dimensional probability distribution functions of the ground state wave function of H_5^+ along R, r_2, and B_1.

In Fig. 3, we give the 2D cuts through the wave functions of the first five vibrationally excited states of H_5^+. For these states, they all have well-defined nodal patterns with only one of the modes being excited. These states are found to have no nodes in any other degrees of freedom. For the $n = 1$ state, as shown in the first row of Fig. 3, it has an excitation of one quantum in the B_1 torsional angle and thus is labeled as (0,0,1). The state $n = 2$ in the second row is also labeled as (0,0,1) but with a different parity as only one quantum of the torsion mode is excited. In the third row, it can be found there exists a nodal plane along the r_2 coordinate and thus we can label it as (0,1,0) which is the fundamental of the central proton hopping mode. The state $n = 4$ presented in the next row corresponds to the first overtone of the torsion mode and is labeled as (0,0,2). There also exists another state $n = 5$ having the same assignment but with a different parity, as shown in the last row of the figure.

The 2D cuts of the wave functions for the 6th–10th excited states are plotted in Fig. 4. For these relatively high-lying excited states, at least two modes are excited. In other words, there exists coupling between different modes. For the 6th excited state, as shown in the first row of Fig. 4, there exists an excitation of one quantum each along the coordinates r_2 and B_1; thus, it is labeled as (0,1,1). Similarly, the $n = 7$ state is labeled as (0,1,1) with a different parity. The $n = 8$ state can be label as (1,1,0) by inspecting the third row.

TABLE V. Vibrational energies of the first 10 excited states of H_5^+ with total angular momentum $J = 0$ with the corresponding ZPE as a reference (in cm^{-1}). The intermolecular vibrational quantum numbers (n_{str}, n_{hop}, n_{tor}) denote the H_2–H_3^+ stretch, the shared-proton hopping, and the out-of-plane torsion, respectively.

	This work			MCTDH[a]	MCTDH[b]
n	Energy	Parity	(n_{str}, n_{hop}, n_{tor})	Energy	Energy
0	0.0 (7214.6)	+1	(0,0,0)	0.0 (7210.3)	0.0 (7202.6)
1	87.3	+1	(0,0,1)	96.3	92.6
2	138.7	−1	(0,0,1)	135.7	133.3
3	354.4	+1	(0,1,0)	358.7	365.4
4	444.0	+1	(0,0,2)	452.9	447.1
5	446.8	−1	(0,0,2)	453.6	452.3
6	447.3	+1	(0,1,1)	464.4	462.8
7	486.3	−1	(0,1,1)	495.1	495.9
8	642.6	+1	(1,1,0)	673.6	679.5
9	736.9	+1	(1,1,1)	784.3	779.5
10	774.3	−1	(1,1,1)	809.4	808.2

[a]Reference 45.
[b]Reference 46.

Obviously, it has an excitation of one quantum each along R and r_2. For the state $n = 9$, as plotted in the fourth row, the three modes have all been excited and it is labeled as (1,1,1). Similarly, the $n = 10$ state can be labeled as (1,1,1) with a different parity.

In the last two columns of Table V, we also present the MCTDH energies of the first 10 excited states of H_5^+ from Refs. 45 and 46 for comparison. Obviously, the two MCTDH calculations with different mode combination scheme (5-mode combination in Ref. 45 vs. 4-mode combination in Ref. 46) give almost the same result, and the difference is within 10 cm^{-1} for all the energies presented. The small difference should be caused by the different n-mode representation of the PES. By comparing our results with the MCTDH values in Ref. 45 (5-mode combination scheme), it can be found that the MCTDH energies agree quite well with our values for the first five vibrationally excited states with the difference no more than 10 cm^{-1}. While for higher vibrational states, the difference becomes a little larger, ranging from 8.8 cm^{-1} for $n = 7$ to 47.4 cm^{-1} for $n = 9$ with the others in between them. It seems that the MCTDH values are systematically larger than ours except for the state $n = 2$, in which the MCTDH value is 3 cm^{-1} smaller than ours. Considering that the approximation of the n-mode representation of the PES included in the MCTDH calculations, the small difference within 47.4 cm^{-1} over the vibrational states studied should be reasonable and acceptable.

In Table V, we could not find the fundamental of the H_2–H_3^+ stretch, (1,0,0), and the first overtone of the shared-proton hopping, (0,2,0), which one would expect to occur around 280 cm^{-1} and 700 cm^{-1}, respectively. A simple explanation can be found in Lin and McCoy's paper.[53] In their work, they used the simple normal mode to local progressions of transitions in the proton-transfer mode and provided alternative assignments of the experimental spectra. They argued that the underlying-motion is no longer normal modes but some type of large-amplitude motion. Thus, according to their explanation, 354.4 cm^{-1} (0,1,0) can be re-assigned as the $\nu = 1$ state in the shared proton chattering mode and 642.6 cm^{-1} (1,1,0) as the $\nu = 2$ state. Indeed, the wave function cut of $n = 3$ in the first column of Fig. 3 shows that it is not a pure r_2 mode but a combination of R and r_2 motion.

The tunneling splitting of the ground-state torsion mode is defined as the difference between the energies of the ground state and the first torsional excited state. In Table VI, we present the ground-state torsional splitting, the fundamental of the proton hopping mode, and the first torsional overtone and compare them with earlier theoretical results where available. In the second row, we list the fundamental of the torsion mode (tunneling splitting) of this work together with those calculated by DMC,[22] MM-RPH,[22] and MCTDH[45,46] methods. It can be seen that our result (87.3 cm^{-1}) is in between the DMC value (80 cm^{-1}) and the MCTDH values (96.3 cm^{-1} in Ref. 45 and 92.6 cm^{-1} in Ref. 46) with 7.3 cm^{-1}

TABLE VI. Comparison of the ground-state torsional splitting, the υ_{H^+} fundamental of H_5^+, and the first overtone of the torsion mode with other theoretical results (in cm^{-1}).

	DMC[a]	MM-RPH[a]	MCTDH[b]	MCTDH[c]	DMC[d]	This work
$\Delta\upsilon_{torsion}$	80	66	96.3	92.6		87.3
υ_{H^+}	334	382	358.7	365.4	369 ± 5	354.4
$2\Delta\upsilon_{torsion}$			452.9	447.1		444.0

[a]Reference 22.
[b]Reference 45.
[c]Reference 46.
[d]Reference 53.

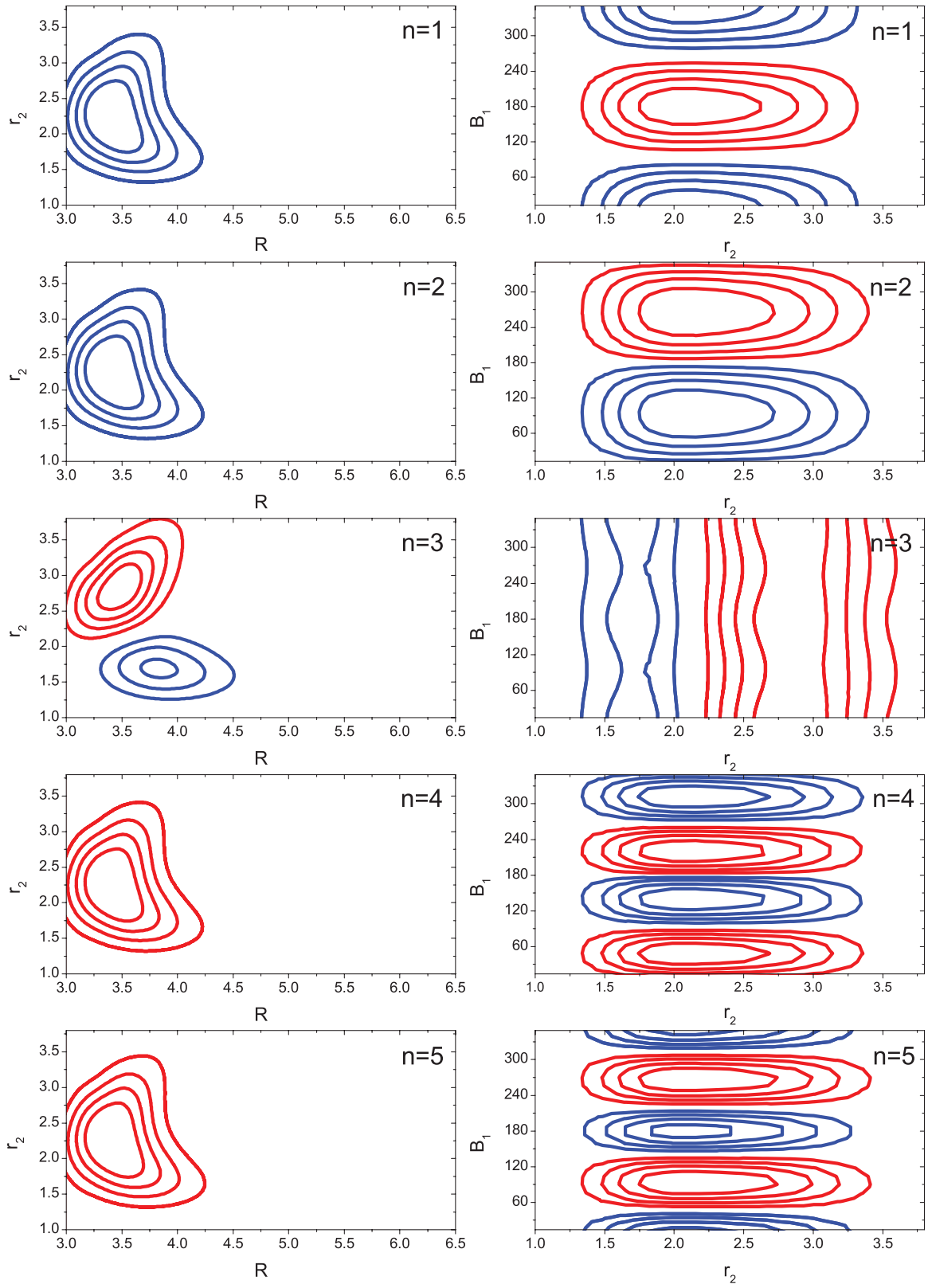

FIG. 3. Cuts through the wave functions of the first five vibrationally excited states of the H_5^+ ion. Other coordinates are fixed at DVR points with maximum amplitude of the corresponding one-dimensional wave function. Contours are from 20% to 80% of the maximum amplitude with an interval of 20%. The red (blue) curves enclose regions of positive (negative) amplitude.

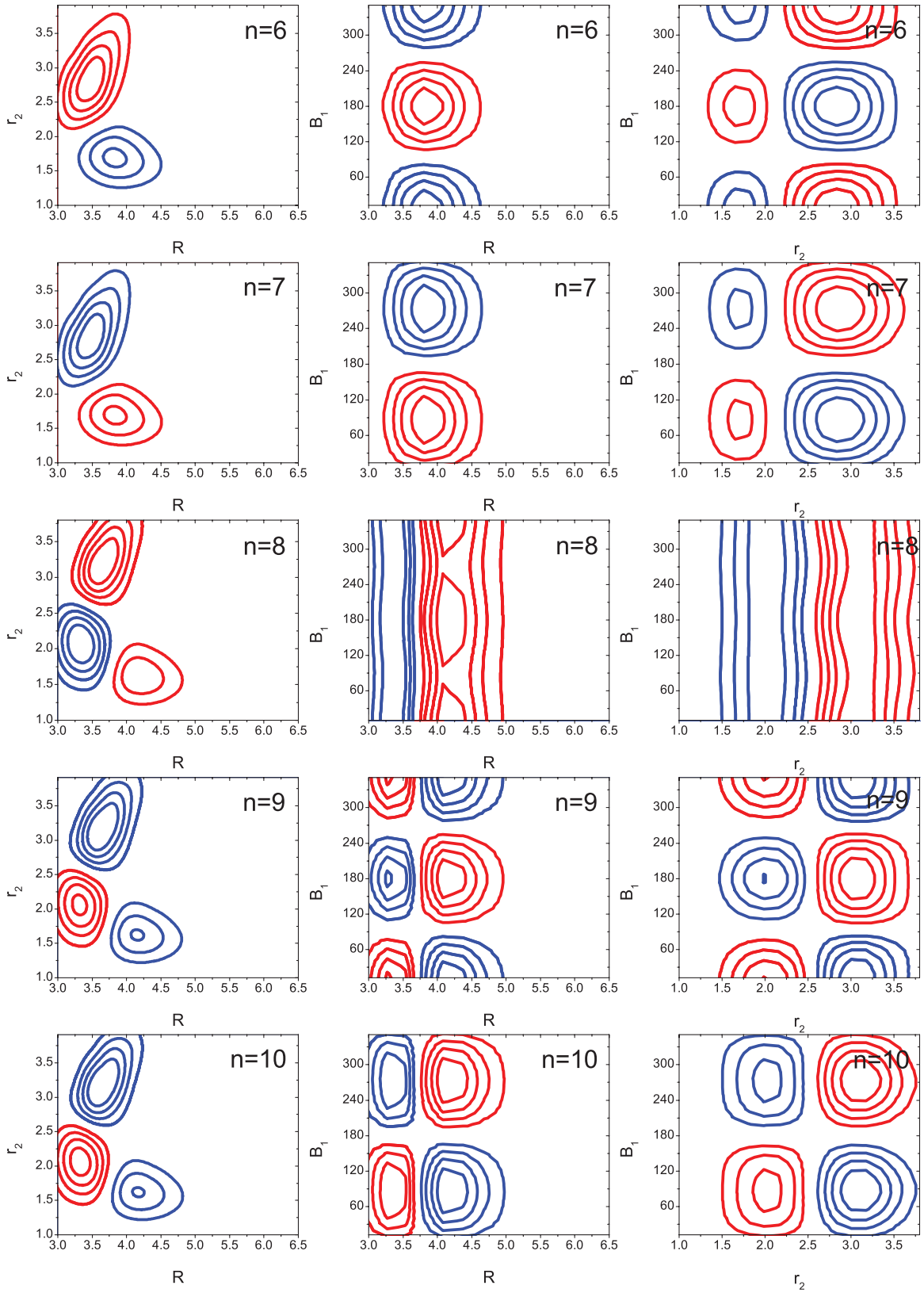

FIG. 4. Cuts through the wave functions of the sixth to tenth vibrationally excited states of the H_5^+ ion. Other coordinates are fixed at DVR points with maximum amplitude of the corresponding one-dimensional wave function. Contours are from 20% to 80% of the maximum amplitude with an interval of 20%. The red (blue) curves enclose regions of positive (negative) amplitude.

larger than the DMC value. The MM-RPH value (66 cm^{-1}) is smaller than the other ones by at least 14 cm^{-1}. Overall, the tunneling splitting from this work is closest to the DMC value.

For the fundamental of the proton hopping mode, as listed in the third row, the two DMC calculations (Refs. 22 and 53) give distinct results, with the value in Ref. 22 being 35 cm^{-1} smaller than in Ref. 53. Here, we should note that Cheng *et al.*[22] employed a slight different PES from the others, which possibly cause the difference between the two DMC calculations. The MCTDH value based on the 4-mode combination scheme[46] is well located in the statistical uncertainties of the DMC energy reported by Lin and McCoy.[53] However, the other three calculations, MM-RPH,[22] MCTDH (5-mode combination scheme),[45] and the present work, all give results that are well outside of the statistical uncertainties of the DMC energy.[53] In addition, the fundamental of the proton hopping mode of this work is close to the MCTDH result in Ref. 45, and the difference between them is only 4.3 cm^{-1}.

In the fourth row, we present the first overtone of the torsion mode obtained from this work and the two MCTDH calculations.[45,46] It can be seen that the two MCTDH energies are close to each other and are slightly larger than our calculated energy.

Through the comparison of vibrational energies among different theoretical methods above, it is clear that the *n*-mode representation of the PES employed in the MCTDH method, at least 5-mode combination scheme and 4-mode combination scheme, works well for the bound state calculations of H_5^+ among this energy range. The DMC approach gives a very good description of the ground state and also of some specific excited states, while the MM-RPH approach generally provides results with a relatively larger difference.

IV. CONCLUSIONS

We have reported rigorous full-dimensional calculations of the vibrational spectra of H_5^+ for the total angular momentum $J = 0$ in a relatively low energy range up to 774.3 cm^{-1}. An accurate global potential energy surface, developed by Xie *et al.*[36] based on extensive high-level *ab initio* calculations, was employed in the calculation. The zero point energies of H_5^+ and its isotopic variants were presented and compared with earlier theoretical results. Good consistency among different methods was found. By inspecting different cuts through the wave functions, the first 10 vibrationally excited states of H_5^+ have been successfully assigned using three quantum numbers (the H_2–H_3^+ stretch, the shared proton hopping, and the out-of-plane torsion). The ground-state torsional tunneling splitting is 87.3 cm^{-1}, the fundamental of the central proton hopping mode is 354.4 cm^{-1}, and the first overtone of the torsion mode is 444.0 cm^{-1}. All these values agree well with the available results from the DMC and MCTDH calculations. However, the MM-RPH calculation provides a slightly smaller value for the torsional tunneling splitting and a relatively larger value for the fundamental of the central proton hopping mode.

At the moment, it is still very challenging to perform full-dimensional quantum-mechanical calculations for H_5^+ without any approximations for the higher vibrational states. The Jacobi coordinates in the work, which is not a set of fully symmetric coordinates, make it unfeasible to implement the permutation symmetry among all identical particles. Some attempts to use symmetric coordinates for calculations are in progress. We hope that this work can offer some useful information to experimentalists, and stimulate more experimental investigations on these highly fluxional hydrogen-bonded cations system.

ACKNOWLEDGMENTS

H. Song, S.-Y. Lee, and M. Lu were supported by a Ministry of Education, Singapore, Grant No. MOE2011-T2-2-087. M. Yang was supported by the National Science Foundation of China (Project Nos. 21221064 and 21073229). The authors would like to thank Professor Joel M. Bowman for helpful discussion and Dr. Yimin Wang for sending us the PES used in this work.

[1] P. Chen, X. Wu, J. Lin, and K. L. Tan, Science **285**, 91 (1999).
[2] D. Gerlich, E. Herbst, and E. Roueff, Planet. Space Sci. **50**, 1275 (2002).
[3] W.-Q. Deng, X. Xu, and W. A. Goddard, Phys. Rev. Lett. **92**, 166103 (2004).
[4] J. T. Hallett, D. E. Shemansky, and X. Liu, Astrophys. J. **624**, 448 (2005).
[5] D. Gerlich, F. Windisch, P. Hlavenka, R. Plašil, and J. Glosik, Philos. Trans. R. Soc. London, Ser. A **364**, 3007 (2006).
[6] P. H. Dawson and A. W. Tickner, J. Chem. Phys. **37**, 672 (1962).
[7] U. A. Arifov, S. L. Pozharov, I. G. Chernov, and Z. A. Mukhamediev, High Energy Chem. **5**, 69 (1971).
[8] S. L. Bennett and F. H. Field, J. Am. Chem. Soc. **94**, 8669 (1972).
[9] K. Hiraoka and P. Kebarle, J. Chem. Phys. **62**, 2267 (1975).
[10] R. Johnsen, C. Huang, and M. A. Biondi, J. Chem. Phys. **65**, 1539 (1976).
[11] R. J. Beuhler, S. Ehrenson, and L. Friedman, J. Chem. Phys. **79**, 5982 (1983).
[12] K. Hiraoka, J. Chem. Phys. **87**, 4048 (1987).
[13] K. Hiraoka and T. Mori, J. Chem. Phys. **91**, 4821 (1989).
[14] M. Okumura, L. I. Yeh, and Y. T. Lee, J. Chem. Phys. **88**, 79 (1988).
[15] Y. K. Bae, Chem. Phys. Lett. **180**, 179 (1991).
[16] K. Giles, N. G. Adams, and D. Smith, J. Phys. Chem. **96**, 7645 (1992).
[17] M. Cordonnier, D. Uy, R. M. Dickson, K. E. Kerr, Y. Zhang, and T. Oka, J. Chem. Phys. **113**, 3181 (2000).
[18] H. Roberts, E. Herbst, and T. J. Millar, Mon. Not. R. Astron. Soc. **336**, 283 (2002).
[19] O. Kornilov and J. P. Toennies, J. Chem. Phys. **128**, 194306 (2008).
[20] E. Hugo, O. Asvany, and S. Schlemmer, J. Chem. Phys. **130**, 164302 (2009).
[21] K. N. Crabtree, C. A. Kauffman, B. A. Tom, E. Becka, B. A. McGuire, and B. J. McCall, J. Chem. Phys. **134**, 194311 (2011).
[22] T. C. Cheng, B. Bandyopadyay, Y. Wang, S. Carter, B. J. Braams, J. M. Bowman, and M. A. Duncan, J. Phys. Chem. Lett. **1**, 758 (2010).
[23] T. C. Cheng, L. Jiang, K. R. Asmis, Y. Wang, J. M. Bowman, A. M. Ricks, and M. A. Duncan, J. Phys. Chem. Lett. **3**, 3160 (2012).
[24] R. Ahlrichs, Theoret. Chim. Acta (Berl.) **39**, 149 (1975).
[25] Y. Yamaguchi, J. F. Gaw, R. B. Remington, and H. F. Schaefer, J. Chem. Phys. **86**, 5072 (1987).
[26] M. Farizon, H. Chermette, and B. Farizon-Mazuy, J. Chem. Phys. **96**, 1325 (1992).
[27] T. Pang, Chem. Phys. Lett. **228**, 555 (1994).
[28] W. P. Kraemer, V. Spirko, and O. Bludský, J. Mol. Spectrosc. **164**, 500 (1994).
[29] I. Štich, D. Marx, M. Parrinello, and K. Terakura, J. Chem. Phys. **107**, 9482 (1997).
[30] H. Müller and W. Kutzelnigg, Phys. Chem. Chem. Phys. **2**, 2061 (2000).
[31] M. Barbatti, G. Jalbert, and M. A. C. Nascimento, J. Chem. Phys. **113**, 4230 (2000).

[32]R. Prosmiti, A. A. Buchachenko, P. Villarreal, and G. Delgado-Barrio, Theor. Chem. Acc. **106**, 426 (2001).
[33]R. Prosmiti, P. Villarreal, and G. Delgado-Barrio, J. Phys. Chem. A **107**, 4768 (2003).
[34]G. E. Moyano and M. A. Collins, J. Chem. Phys. **119**, 5510 (2003).
[35]Y. Ohta, J. Ohta, and K. Kinugawa, J. Chem. Phys. **121**, 10991 (2004).
[36]Z. Xie, B. J. Braams, and J. M. Bowman, J. Chem. Phys. **122**, 224307 (2005).
[37]V. Špirko, T. Amano, and W. P. Kraemer, J. Chem. Phys. **124**, 224303 (2006).
[38]G. M. e Silva, R. Gargano, W. B. da Silva, L. F. Roncaratti, and P. H. Acioli, Int. J. Quantum Chem. **108**, 2318 (2008).
[39]P. H. Acioli, Z. Xie, B. J. Braams, and J. M. Bowman, J. Chem. Phys. **128**, 104318 (2008).
[40]A. Aguado, P. Barragán, R. Prosmiti, G. Delgado-Barrio, P. Villarreal, and O. Roncero, J. Chem. Phys. **133**, 024306 (2010).
[41]R. P. de Tudela, P. Barragán, R. Prosmiti, P. Villarreal, and G. Delgado-Barrio, J. Phys. Chem. A **115**, 2483 (2011).
[42]P. Barragán, R. P. de Tudela, R. Prosmiti, P. Villarreal, and G. Delgado-Barrio, Phys. Scr. **84**, 028109 (2011).
[43]B. A. McGuire, Y. Wang, J. M. Bowman, and S. L. Widicus Weaver, J. Phys. Chem. Lett. **2**, 1405 (2011).
[44]F. Meng, T. Wang, and D. Wang, J. Chem. Phys. **135**, 114307 (2011).
[45]A. Valdés, R. Prosmiti, and G. Delgado-Barrio, J. Chem. Phys. **136**, 104302 (2012).
[46]A. Valdés, R. Prosmiti, and G. Delgado-Barrio, J. Chem. Phys. **137**, 214308 (2012).
[47]K. Park and J. C. Light, J. Chem. Phys. **126**, 044305 (2007).
[48]D. Wang, Z. Xie, and J. M. Bowman, J. Chem. Phys. **132**, 084305 (2010).
[49]C. Sanz-Sanz, O. Roncero, A. Valdés, R. Prosmiti, G. Delgado-Barrio, P. Villarreal, P. Barragán, and A. Aguado, Phys. Rev. A **84**, 060502(R) (2011).
[50]K. N. Crabtree, B. A. Tom, and B. J. McCall, J. Chem. Phys. **134**, 194310 (2011).
[51]A. Aguado, C. Sanz-Sanz, P. Villarreal, and O. Roncero, Phys. Rev. A **85**, 032514 (2012).
[52]P. Barragán, R. Prosmiti, O. Roncero, A. Agudo, P. Villarreal, and G. Delgado-Barrio, J. Chem. Phys. **133**, 054303 (2010).
[53]Z. Lin and A. B. McCoy, J. Phys. Chem. Lett. **3**, 3690 (2012).
[54]D. Wang, J. Chem. Phys. **124**, 201105 (2006).
[55]J. Echave and D. C. Clary, Chem. Phys. Lett. **190**, 225 (1992).
[56]D. Wang, J. Chem. Phys. **119**, 12057 (2003).
[57]R. Lehoucq, D. C. Sorensen, and C. Yang, Arpack user's guide: Solution of large-scale eigenvalue problems with implicitly restarted Arnoldi methods 1998, see http://www.caam.rice.edu/software/ARPACK.
[58]M. Abramowitz and I. A. Stegun, *Handbook of Mathematical Functions: With Formulas, Graphs, and Mathematical Tables* (Dover, 1972).
[59]S. Carter, S. J. Culik, and J. M. Bowman, J. Chem. Phys. **107**, 10458 (1997).
[60]S. Carter, J. M. Bowman, and N. C. Handy, Theor. Chem. Acc. **100**, 191 (1998).
[61]J. M. Bowman, S. Carter, and X. Huang, Int. Rev. Phys. Chem. **22**, 533 (2003).
[62]M. Mandziuk and Z. Bačić, J. Chem. Phys. **98**, 7165 (1993).
[63]D. H. Zhang, Q. Wu, J. H. Zhang, M. von Dirke, and Z. Bačić, J. Chem. Phys. **102**, 2315 (1995).